131.2, 121.5, 113.5, 113.2, 71.9, 71.1, 69.5, 59.1, 55.4; FTIR (neat film): $\tilde{\nu}$ = 2888 (w), 1614 (s), 1445 (s), 1241 (w), 1100 (w), 811 (s) $cm^{-1}$; HRMS (MALDI): *m/z*: calcd for $C_{27}H_{34}NO_6$ [$M+H^+$] 468.2381; found 468.2370; TLC $R_f$ (55% EtOAc/Hex) 0.20.

Received: December 18, 2000 [Z16296]


[1] a) A. P. de Silva, D. B. Fox, A. J. M. Huxley, T. S. Moody, *Coord. Chem. Rev.* **2000**, *205*, 41 – 57; b) L. Prodi, F. Bolletta, M. Montalti, N. Zaccheroni, *Coord. Chem. Rev.* **2000**, *205*, 59 – 83; c) V. Amendola, L. Fabbrizzi, M. Licchelli, C. Mangano, P. Pallavicini, L. Parodi, A. Poggi, *Coord. Chem. Rev.* **2000**, *192*, 649 – 669; d) A. P. de Silva, D. B. Fox, A. J. M. Huxley, N. D. McClenaghan, J. Roiron, *Coord. Chem. Rev.* **1999**, *186*, 297 – 306; e) J. P. Desvergne, A. W. Czarnik, *NATO ASI Ser. Ser. C* **1997**, *492* ; f) A. W. Czarnik, *ACS Symp. Ser.* **1993**, *538*.

[2] For select recent examples, see: a) Y. Kawanishi, K. Kikuchi, H. Takakusa, S. Mizukami, Y. Urano, T. Higuchi, T. Nagano, *Angew. Chem.* **2000**, *112*, 3580 – 3582; *Angew. Chem. Int. Ed.* **2000**, *39*, 3438 – 3440; b) S. Deo, H. A. Godwin, *J. Am. Chem. Soc.* **2000**, *122*, 174 – 175; c) A. P. de Silva, J. Eilers, G. Zlokarnik, *Proc. Natl. Acad. Sci. USA* **1999** *96*, 8336 – 8337.

[3] We have recently characterized binding-induced conformational restriction of biaryl fluorophores as an efficient chemosensor signalling mechanism: S. A. McFarland, N. S. Finney, *J. Am. Chem. Soc.* in press. For a previous example in which formation of a 2:2 ligand/$K^+$ restricts energy-wasting olefin isomerization in a stilbenoid fluorophore, see: W.-S. Xia, R. H. Schmehl, C.-J. Li, *J. Am. Chem. Soc.* **1999**, *121*, 5599 – 5600.

[4] Quantum yields were determined by standard methods (J. R. Lakowicz, *Principles of Fluorescence Spectroscopy*, 2nd ed., Kluwer, New York, **1999**). The quantum yields of **2** and **3** are 0.027 and 0.024, respectively, using tryptophan in $H_2O$ as a standard ($\phi = 0.13$). We estimate values of $\phi$ to be accurate to $\pm 25\%$. The excitation maximum for the LE state is 290 nm; the excitation maximum for the CT band is 345 nm.

[5] For a review of fluorescent chemosensors based on induced charge transfer, see: B. Valeur, I. Leray, *Coord. Chem. Rev.* **2000**, *205*, 3 – 40.

[6] As detailed in our previous analysis of biphenyl-derived fluorescent chemosensors,[3] we reason as follows: no changes are observed in the UV spectrum upon complexation of $Li^+$, suggesting that the excitation probability (Einstein *A* coefficient), and thus the emission probability (Einstein *B* coefficient) and the rate of radiative decay ($k_r$), remain constant; the energetic separation of the $S_1$ and $S_0$ potential energy surfaces is sufficient (> 60 kcal $mol^{-1}$) to preclude internal conversion ($k_{ic} \approx 0$); increased quantum yield must thus arise from decreased intersystem crossing (ISC); $k_{ISC}$ is known to increase with dihedral angle, and binding-induced conformational restriction thus leads to reduction in $k_{ISC}$.

[7] Association constants were determined by nonlinear least-squares fitting of lg[metal] versus $I/I_0$ plots. Curve fitting was carried out with the Prism3 software package (Graphpad, Inc., San Diego, CA). The reported $K_a$ values have 95% confidence limits of $\pm 0.1$ lg $K_a$ units. In all cases reported here curve fitting is consistent with the formation of 1:1 metal/ligand complexes.

[8] Titration of **2** – **4** with $Na^+$ or $K^+$ does not lead to appreciable change in fluorescence emission.

[9] Both **2** and **3** respond slowly to $Mg^{2+}$. In the case of **3**, the hysteresis is severe enough to make $K_a$ determination impractical. We tentatively ascribe the differences in the responses of **2** and **3** to coordination of $Li^+$ and $Ca^{2+}$ by the distal oxygen atoms of the ether chain, although details of these interactions remain to be elucidated.

[10] a) R. M. Izatt, K. Pawlak, J. S. Bradshaw, R. L. Bruening, *Chem. Rev.* **1991**, *91*, 1721 – 2085; b) R. M. Izatt, K. Pawlak, J. S. Bradshaw, R. L. Bruening, *Chem. Rev.* **1995**, *95*, 2529 – 2586.

[11] For recent examples in which metal ion coordination has been used to "tune" fluorescence emission, see: a) H. S. Joshi, R. Jamshidi, Y. Tor, *Angew. Chem.* **1999**, *111*, 2887 – 2891; *Angew. Chem. Int. Ed.* **1999**, *38*, 2722 – 2725; b) J. C. Loren, J. S. Siegel, *Angew Chem.* **2001**, *113*, 776 – 779; *Angew. Int. Ed. Engl.* **2001**, *40*, 754 – 757.

[12] Despite the desirability of the approach, combinatorial libraries of small-molecule fluorescent chemosensors have received limited attention. See: a) A. W. Czarnik, *Chem. Biol.* **1995**, *2*, 423 – 428; b) C. T. Chen, H. Wagner, W. C. Still, *Science* **1998**, *279*, 851 – 853; c) S. E. Schneider, S. N. O'Neil, E. V. Anslyn, *J. Am. Chem. Soc.* **2000**, *122*, 542 – 543; d) F. Szurdoki, D. Ren, D. R. Walt, *Anal. Chem.* **2000**, *72*, 5250 – 5257.

[13] A. F. Littke, C. Y. Dai, G. C. Fu, *J. Am. Chem. Soc.* **2000**, *122*, 4020 – 4028.


# Benzylic Imine Catenates: Readily Accessible Octahedral Analogues of the Sauvage Catenates**

David A. Leigh,* Paul J. Lusby, Simon J. Teat, Andrew J. Wilson, and Jenny K. Y. Wong

Historically, one of the triumphs of coordination chemistry has been its application to the synthesis of mechanically interlocked molecular architectures, that is catenanes, rotaxanes, and knots.[1–10] In 1984 Sauvage et al. used the preferred tetrahedral geometry of $Cu^I$ to organize appropriately derivatized phenanthroline ligands into a fixed mutually orthogonal orientation, whereupon a double macrocyclization reaction gave the [2]catenate in 27% yield (Scheme 1a).[2]

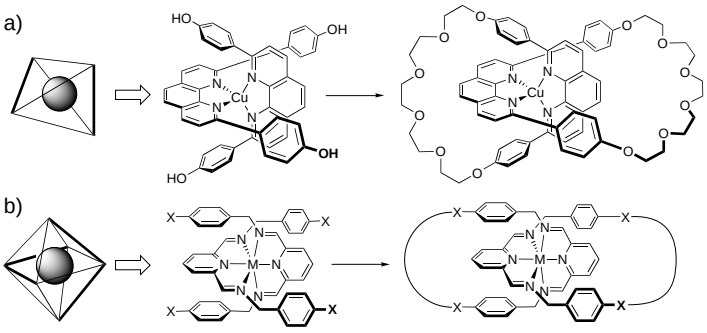


Scheme 1. Synthesis of catenates by orthogonalization of coordinated ligands about metal templates with a) tetrahedral and b) octahedral coordination preference. M in (b): $Mn^{2+}$, $Fe^{2+}$, $Co^{2+}$, $Ni^{2+}$, $Cu^{2+}$, $Zn^{2+}$, $Cd^{2+}$, $Hg^{2+}$.


[*] Prof. D. A. Leigh, Dr. P. J. Lusby, A. J. Wilson, J. K. Y. Wong
Centre for Supramolecular and Macromolecular Chemistry
Department of Chemistry, University of Warwick
Coventry CV4 7AL (UK)
Fax: (+44) 24-7652-3258
E-mail: David.Leigh@Warwick.ac.uk
Dr. S. J. Teat
CCLRC Daresbury Laboratory
Warrington (UK)



[**] This work was supported by the EPSRC. D.A.L. is an EPSRC Advanced Research Fellow (AF/982324). We thank Dr. B. P. Murphy (Manchester Metropolitan University) for useful discussions and Drs. T. J. Kidd, S. M. Lacy (University of Warwick), G. Di Orazio and R. Nasreen (University of Manchester, Institute of Science and Technology) for early ligand design.


Supporting information for this article is available on the WWW under http://www.angewandte.com or from the author.

Subsequent studies on the system boosted yields to near quantitative levels (by ring closing metathesis, RCM)[3] and extended the interlocked architectures available to [*n*]catenates ($n = 2-8$),[4] catenands (the demetalated, but still interlocked ligands),[5] rotaxanes,[6] pseudo-rotaxanes,[7] and knots.[8] Interlocked ligands can have remarkable properties; catenates are amongst the most stable complexes of $Cu^{I}$ that exist with a neutral ligand,[5] and catenands also stabilize[9] the ordinarily disfavored tetrahedral geometries of $Ni^{I}$ and $Cu^{0}$. However, although other metals have been introduced[9] and alternative trigonal-bipyrimidal "stations" employed in redox-switchable systems,[10] the basic catenate assembly system based on a low oxidation state, tetrahedrally coordinated metal template and phenanthroline ligands has remained largely unchanged. Expanding this elegant strategy to include catenates with higher oxidation state, octahedrally coordinated metal centers is of obvious appeal (Scheme 1 b),[11] and pioneering work in this regard has been carried out by Schröder et al.,[12] Busch et al.,[13] and others,[1d, 14] yet only two octahedral catenates[1d, 14] (and two knots[15, 16]) have been described to date. Catenanes assembled by hydrogen bonds can exhibit a continuous range of (tunable) dynamic properties,[17, 18] but the strong coordination bonds present in catenates lock the macrocyclic components in fixed positions whereas, in the absence of the metal, these rings rotate with virtually complete (but uncontrolled) freedom. The difference in the type of dynamics available to each system led us to seek a route to catenates of a size and shape that would be both compatible and interchangeable in molecular devices with benzylic amide catenanes assembled by hydrogen bonds (e.g. **I**).

The basic architecture of benzylic amide macrocycles is rather well suited to adapting to other sorts of assembly processes (Scheme 2). The rigid framework positions multiple donor groups such that they converge towards the center of the cavity, while the isophthalic spacer holds the aromatic rings in a parallel arrangement at a distance ideal for π stacking with an orthogonally bound guest. The 1,3-linked benzylic motif ensures a complete 180° turn for each fragment (in comparison to, say, the 120° turn for a diphenylphenanthroline unit) holding the endgroups in positions that promote intracomponent rather than intercomponent cyclizations.[19] Thus, the only changes necessary to obtain a system based on metal ion chelation (i.e. arriving at complexes with the benzylic bis(2,6-diiminopyridine)catenand ligand **1**) was to replace the amide groups with imine groups and, for stability reasons, the phenolic esters with ethers (Scheme 2).

The zinc(II) perchlorate complex $[Zn\mathbf{2}_2](ClO_4)_2$ was isolated as a precipitate in 83% yield from simple addition of a solution of the Schiff base ligand **2**[20] in dichloromethane to a methanolic solution of $Zn(ClO_4)_2 \cdot 6H_2O$. Imines are one of the few classes of substrates not normally compatible with olefin metathesis (indeed, the free Schiff-base ligand **2** cannot be converted into the macrocycle by RCM). However, precoordination ties up the imine groups and the tetraolefin complex $[Zn\mathbf{2}_2](ClO_4)_2$ smoothly underwent double macrocyclization by RCM with Grubbs' catalyst ([Ru(=CHPh)-$(PCy_3)_2Cl_2$], $CH_2Cl_2$, Ar, RT, 4 h) to give the zinc(II) catenate $[Zn\mathbf{1}](ClO_4)_2$ in 73% yield as a mixture of *E*,*E*, *E*,*Z*, and *Z*,*Z* diastereomers (Scheme 2 a). Exposure of the reaction mixture to the metathesis catalyst for four days equilibrated the products to give almost exclusively the *E*,*E* isomer.

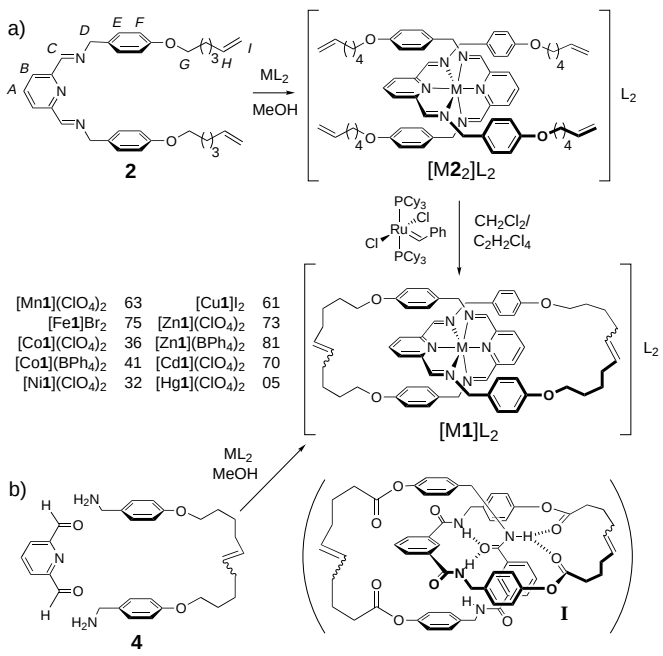


Scheme 2. Synthesis of benzylic imine catenates $[M\mathbf{1}]L_2$ by a) double macrocyclization of a preformed octahedral complex $[M\mathbf{2}_2]L_2$, b) spontaneous metal-promoted assembly of nonchelated precursors. The yields (in %) refer to route (a); the yields from route b are not yet optimized, but are uniformally higher. The ligand design is based on that of benzylic amide catenanes, e.g. **I**.[17b]

In contrast to the situation with the classic tetrahedral phenanthroline system, the same catenate $[Zn\mathbf{1}](ClO_4)_2$ could also be prepared by assembling the coordinating sites in situ (Scheme 2 b). Treatment of the bis-amine **4**[21] with 2,6-pyridinedicarbaldehyde and $Zn(ClO_4)_2 \cdot 6H_2O$ in methanol resulted in the precipitation of the (*E*,*E*)-catenate after one hour in 53% yield. In this case, the metal center orders the construction of the catenate about itself, through the reversible formation of four imine bonds from five components, as the lowest energy means by which it can satisfy its desired octahedral coordination geometry.

The $^1H$ NMR spectra of free ligand **2**, zinc(II) precursor complex $[Zn\mathbf{2}_2](ClO_4)_2$, and zinc(II) catenate $[Zn\{(E,E)\text{-}\mathbf{1}\}](ClO_4)_2$ are shown in Figure 1 a–c. Shielding of the benzylic aromatic rings ($H_E$, $H_F$) in both the precursor complex (Figure 1 b) and the catenate (Figure 1 c) with respect to the free ligand (Figure 1 a) is indicative of the entwined (in the case of $[Zn\mathbf{2}_2]L_2$) or interlocked (in the case of $[Zn\{(E,E)\text{-}\mathbf{1}\}]L_2$) architectures. Interestingly, subtle but significant differences take place in the shifts of all the non-alkyl chain resonances between $[Zn\{(E,E)\text{-}\mathbf{1}\}]L_2$ and $[Zn\mathbf{2}_2]L_2$, indicating that a certain amount of reorganization of the ligands needs to occur during catenate formation.

Single crystals suitable for investigation by X-ray crystallography using a synchrotron source were obtained from slow vapor diffusion of diethyl ether into a solution of $[Zn\{(E,E)\text{-}\mathbf{1}\}](ClO_4)_2$ in acetonitrile.[22] The crystal structure (Figure 2) confirms the interlocked molecular architecture, the octahedral geometry around the coordinated zinc and the *E* configuration of the olefinic bonds in both rings. The benzylic

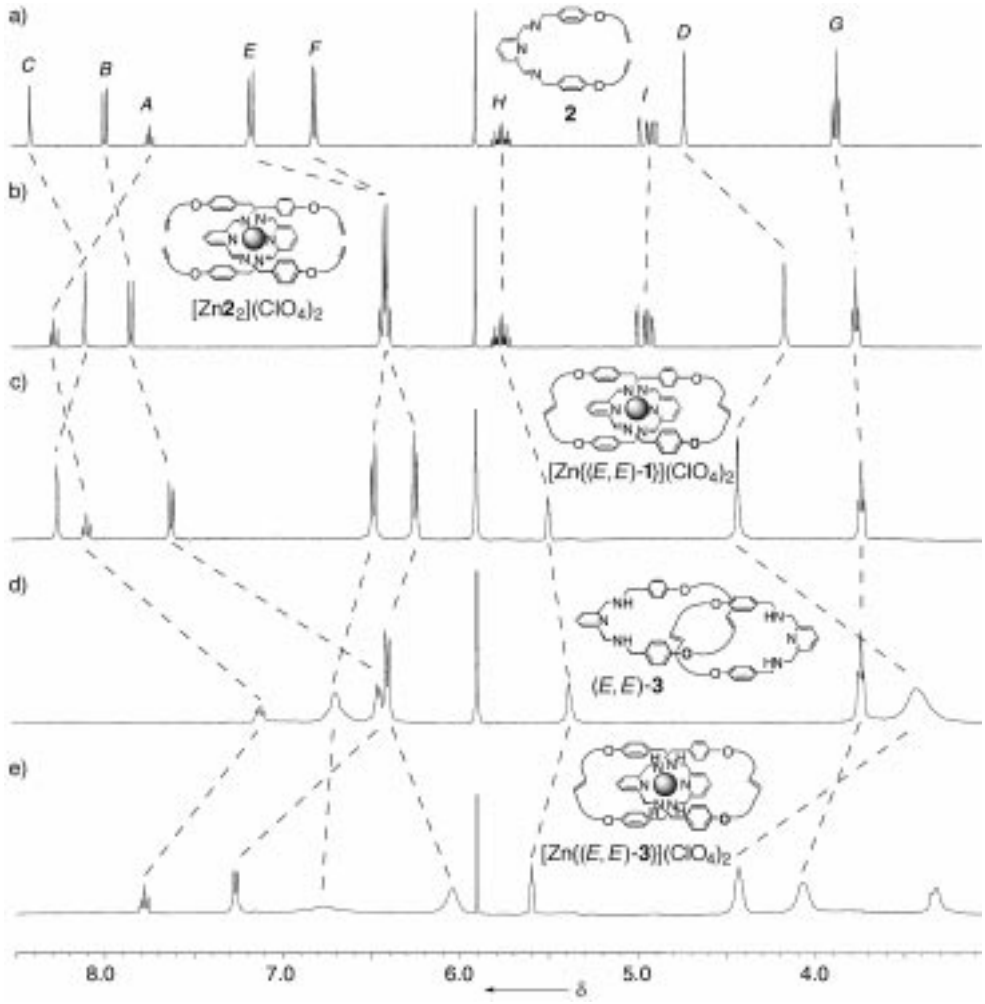


Figure 1. $^1$H NMR spectra (400 MHz, $C_2D_2Cl_4$, 298 K) of a) free Schiff-base ligand **2**, b) acyclic tetraolefin precursor complex $[Zn\mathbf{2}_2](ClO_4)_2$, c) benzylic imine catenate $[Zn\{(E,E)\text{-}\mathbf{1}\}](ClO_4)_2$, d) free benzylic amine catenand $(E,E)$-**3**, and e) benzylic amine catenate $[Zn\{(E,E)\text{-}\mathbf{3}\}](ClO_4)_2$. The assignments correspond to the lettering shown in Scheme 2 for compound **2**.

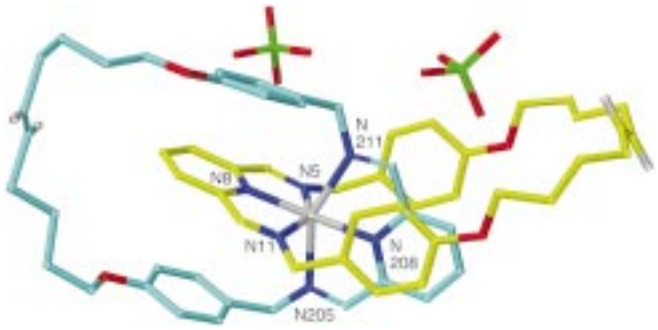


Figure 2. Structure of $[Zn\{(E,E)\text{-}\mathbf{1}\}](ClO_4)_2$ as determined by X-ray crystallography.[22] Carbon atoms of one macrocycle are shown in light blue and those of the other in yellow; oxygen atoms are red, nitrogen dark blue, chlorine green, hydrogen white, and zinc silver. Non-olefinic hydrogen atoms and a molecule of acetonitrile are omitted for clarity. Selected bond lengths [Å]: Zn-N5 2.289, Zn-N8 2.048, Zn-N11 2.211, Zn-N205 2.264, Zn-N208 2.045, Zn-N211 2.276; other selected interatomic distances [Å]: N5-N11 4.348, N8-N208 4.081, N205-N211 4.388; ligand bite angles [°]: N5-Zn-N11 150.14, N205-Zn-N211 150.34.

groups of each macrocycle π-stack with the 2,6-diiminopyridine groups of the other interlocked ring, an interaction which is also clearly present in the precursor complex $[Zn\mathbf{2}_2]L_2$ in halogenated solvents (see NMR data in Figure 1) and doubtless contributes to intracomponent rather than intercomponent cyclization occurring during RCM. Metal coordination necessarily buries the polar imine groups at the center of the molecular structure with the alkyl chains to the outside; a similar overall co-conformation to that observed in the solid state for amphiphilic benzylic amide catenanes.[17a]

The bite angle of the ligand in $[Zn\{(E,E)\text{-}\mathbf{1}\}](ClO_4)_2$ is slightly smaller (150°) than in nonmacrocyclic bis(2,6-diiminopyridine) complexes with $Zn^{II}$[13] (151°) and $Ni^{II}$[12, 13] (151 – 156°), indicating that the ligand is able to adapt to the demands of its environment. Encouraged, we investigated the tolerance of the octahedral catenate assembly system by extending the RCM approach to metals both across and down the periodic table with respect to zinc (i.e. Mn ← Zn and Zn → Hg). The results (see Scheme 2) were uniformally satisfying with the precursor complexes and catenates obtained in each case, often in good yields despite the mixture of diastereomers complicating the purification process.[23] Preliminary studies show that the same catenates are also readily produced by the direct imine bond formation route (Scheme 2b). The crystal structures of two of these new catenates, $[Cu\{(E,E)\text{-}\mathbf{1}\}](ClO_4)_2$ and $[Co\{(E,E)\text{-}\mathbf{1}\}]I_2$, were obtained by using a synchrotron radiation source (Figure 3). The bite angles in these catenates proved larger than in the zinc system (152.1 and 152.7° (Cu), 152.9 and 154.5° (Co)) in line with observed trends with acyclic ligands, confirming the geometrical flexibility of the benzylic bis(2,6-diiminopyridine)catenand ligand system. Interestingly, all the catenates are much more thermally stable than the corresponding precursor complexes. Whilst the acyclic coordination compounds $[M\mathbf{2}_2]L_2$ typically possess sharp melting points in the range 221 – 252 °C, the analogous $[M\mathbf{1}]L_2$ catenates tend to gradually lose color and decompose at temperatures in excess of 350 °C.

The properties of the zinc(II) catenate $[Zn\{(E,E)\text{-}\mathbf{1}\}](ClO_4)_2$ were investigated in more detail (Scheme 3). By single-phase or biphasic extraction of $[Zn\{(E,E)\text{-}\mathbf{1}\}](ClO_4)_2$ in various organic solvents (DMF, $CHCl_3/H_2O$, etc.) with up to 100 equivalents of EDTA, disodium salt, no signs of demetalating the catenate were obtained, suggesting that the

  0044-8249/01/11308-1588 $ 17.50+.50/0 

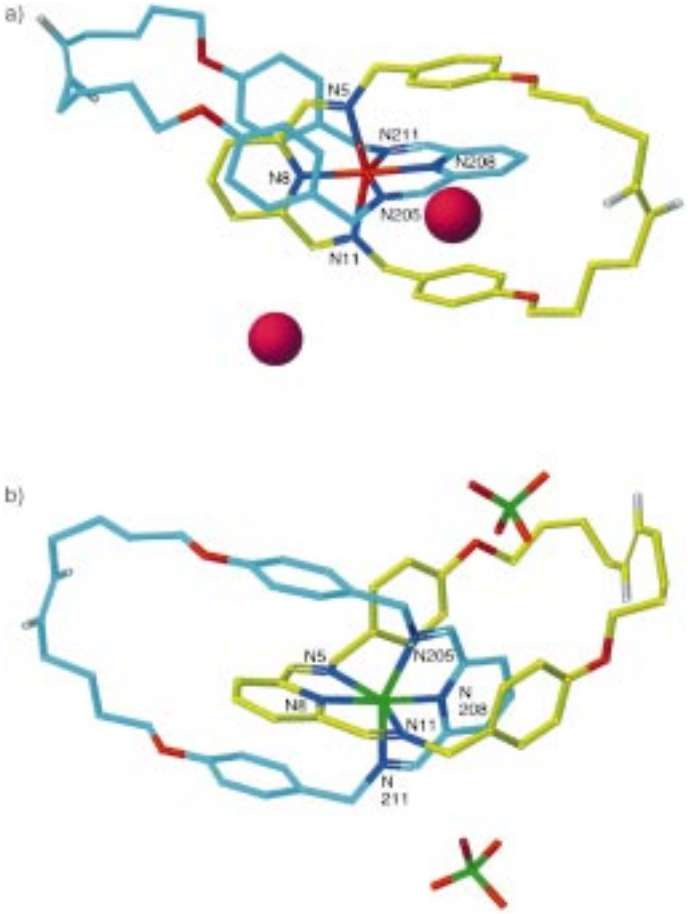


Figure 3. Structures of a) [Co{(*E*,*E*)-**1**}]$I_2$ and b) [Cu{(*E*,*E*)-**1**}]$(ClO_4)_2$ as determined by X-ray crystallography.[22] Color code as in Figure 2, cobalt red, copper green, iodide purple. Non-olefinic hydrogen atoms are omitted for clarity. Ligand bite angles [°]: N5-Co-N11 152.9, N205-Co-N211 154.5; N5-Cu-N11 152.1, N205-Cu-N211 152.7.

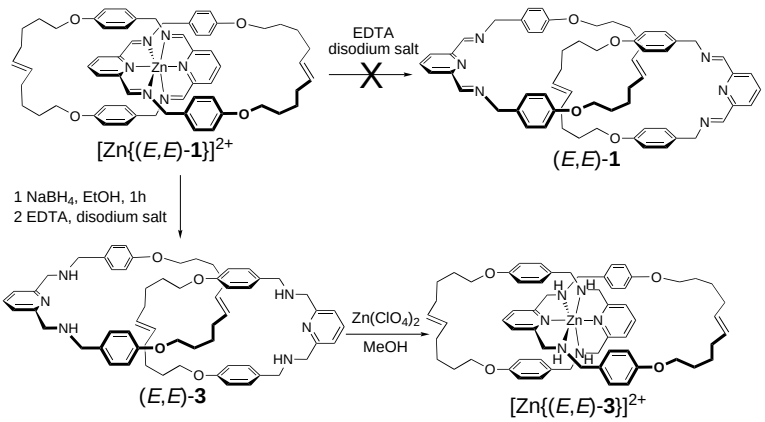


Scheme 3. The chemistry of the octahedral metal catenate [Zn{(*E*,*E*)-**1**}]$(ClO_4)_2$. Direct demetalation is unsuccessful, but reduction of the imine groups allows extraction of the zinc to yield the free benzylic amine catenand (*E*,*E*)-**3** (78%). Remetalation affords the benzylic amine catenate [Zn{(*E*,*E*)-**3**}]$(ClO_4)_2$ (ca. 100%).

combination of the directional, planar diiminopyridyl coordinating motif and the tight, encapsulated architecture provides exceptional kinetic stability. However, reduction of the imine groups followed by washing with aqueous EDTA, disodium salt, resulted in the free benzylic amine catenand (*E*,*E*)-**3**. Remetallation proceeded smoothly to give the corresponding, clearly more labile, benzylic amine catenate [Zn{(*E*,*E*)-**3**}]$(ClO_4)_2$. The $^1$H NMR spectra of (*E*,*E*)-**3** and [Zn{(*E*,*E*)-**3**}]$(ClO_4)_2$ are shown in Figure 1d and e, respectively. The compact nature of the free ligand (*E*,*E*)-**3** is convincingly demonstrated by the shielding of several resonances compared to the acyclic ligand **2**. Protons $H_E$ and $H_F$, for example, which intrinsically should be relatively unaffected by imine reduction, are shifted in (*E*,*E*)-**3** by a similar magnitude to those in the [Zn({*E*,*E*)-**1**}]$(ClO_4)_2$ catenate and the [Zn**2**$_2$]$(ClO_4)_2$ precursor complex despite no directed intercomponent interactions being present between the macrocycles in the catenand. The broad appearance of several resonances in the spectrum of the catenand is probably due to co-conformational exchange processes that are not fast on the NMR time scale at room temperature. The broadened peaks in the spectrum of the amine catenate [Zn{(*E*,*E*)-**3**}]$L_2$, however, may be a result of multiple asymmetric centers being produced by coordination of the four nitrogen atoms which are prochiral in the free ligand **3**.

In conclusion, a simple, versatile and effective route exists to octahedrally coordinated analogues of the Sauvage catenates. This route should be extendable to the synthesis of other metal-based interlocked architectures (such as rotaxanes, shuttles, and knots), and the octahedrally coordinated catenates should be interchangeable in possible molecular devices with catenanes assembled by hydrogen bonds. Catenates are not only a means of stabilizing unusual oxidation states and normally disfavored geometries, but could also find uses in areas where complexes with particularly high kinetic stabilities are required, such as radiotherapy[24] and magnetic resonance imaging,[25] because of the wide range of metals that can adopt octahedral coordination patterns. Finally, we are well aware that metal complexes of 2,6-diiminopyridine ligands also form an important new generation of non-metallocene olefin polymerization catalysts[26] and that intertwined versions of such structures exhibit novel forms of columnar liquid crystalline behavior.[27] The possible application of translationally switchable mechanically interlocked architectures (containing unsaturated metal centers in the case of potential polymerization catalysts) to these areas should be fascinating.

*Experimental Section*

Route (a) of Scheme 2 (RCM): Grubbs' metathesis catalyst [Ru(=CHPh)$(PCy_3)_2Cl_2$] (0.02 g, 0.0243 mmol, 20 mol%) was placed in a sealed, argon-purged, flame-dried Schlenk tube, and subjected to a constant stream of argon for ten minutes. A degassed and argon-purged solution of the [M**2**$_2$]$L_2$ complex (0.122 mmol) in anhydrous dichloromethane (500 mL) was transferred to the Schlenk tube by injection over ten minutes. Reaction was allowed to continue until all the starting material was consumed as evidenced by TLC (typically 4 h), or, in order to maximize the amount of *E*,*E* diastereomer, for 4 days. The resulting solution was evaporated to dryness and purified by repeated chromatography (silica gel, 1–5% MeOH in $CH_2Cl_2$ as eluent) to give the catenates [M**1**]$L_2$ as variously colored solids. Selected data for [Zn{(*E*,*E*)-**1**}]$(ClO_4)_2$: yield: 112 mg, 73%; m.p. 350°C (decomp); $^1$H NMR (400 MHz, [$D_6$]DMSO): $\delta = 1.58$ (m, 8H, $CH_2$), 1.74 (m, 8H, $CH_2$), 2.12 (m, 8H, $CH_2CH$=CH), 3.85 (t, 8H, $J$ =

6.5 Hz, $H_G$), 4.49 (br s, 8H, $H_D$), 5.61 (t, 4H, $J = 3.0$ Hz, $H_H$), 6.36 (AA′BB′ system, 8H, $J = 8.0$ Hz, $H_E$), 6.53 (AA′BB′ system, 8H, $J = 8.0$ Hz, $H_F$), 7.70 (d, 4H, $J = 8.0$ Hz, $H_B$), 8.42 (t, 2H, $J = 8.0$ Hz, $H_A$), 8.50 (s, 4H, $H_C$); $^{13}$C NMR (100 MHz, [D$_6$]DMSO): $\delta = 25.89$, 28.05, 31.50, 60.76, 67.17, 113.91, 127.02, 129.34, 129.97, 130.62, 144.37, 145.25, 158.24, 160.27, FAB-MS (*m*BNA matrix): *m*/*z*: 1126 $[M - ClO_4^-]^+$; anal. calcd for: $C_{62}H_{70}O_{12}N_6Cl_2Zn$ (1225): C 60.73, H 5.71, N 6.86%, found: C 60.46, H 5.97, N 6.67%.

Route (b) of Scheme 2: A solution of 2,6-pyridinedicarbaldehyde (0.97 g, 7.2 mmol) in methanol (10 mL) was added dropwise over 30 min to a solution of bis-amine **4** (7.2 mmol) and metal salt ($ML_2$, 3.6 mmol) in methanol (10 mL). The reaction mixture was stirred at room temperature for 1 h after which time the [M**1**]$L_2$ catenate could either be isolated as a precipitate by filtration, or the solvent removed under reduced pressure and the resulting solid purified as for the RCM procedure.

Received: August 14, 2000
Revised: February 5, 2001 [Z15632]

[1] a) *Molecular Catenanes, Rotaxanes and Knots* (Eds.: J.-P. Sauvage, C. Dietrich-Buchecker), Wiley-VCH, Weinheim, **1999**; for catenanes based on coordination bonds other than the Sauvage catenates see: b) G.-J. M. Gruter, F. J. J. de Kanter, P. R. Markies, T. Nomoto, O. S. Akkerman, F. Bicklehaupt, *J. Am. Chem. Soc.* **1993**, *115*, 12179–12180; c) M. Fujita, F. Ibukuro, H. Hagihara, K. Ogura, *Nature* **1994**, *367*, 720–723; d) C. Piguet, G. Bernardinelli, A. F. Williams, B. Bocquet, *Angew. Chem.* **1995**, *107*, 618–621; *Angew. Chem. Int. Ed. Engl.* **1995**, *34*, 582–584; e) D. M. P. Mingos, J. Yau, S. Menzer, D. J. Williams, *Angew. Chem*. **1995**, *107*, 2045–2047; *Angew. Chem. Int. Ed. Engl*. **1995**, *34*, 1894–1895; f) A. C. Try, M. M. Harding, D. G. Hamilton, J. K. M. Sanders, *Chem. Commun.* **1998**, 723–724; g) D. Whang, K.-M. Park, J. Heo, P. Ashton, K. Kim, *J. Am. Chem. Soc.* **1998**, *120*, 4899–4900; h) C. P. McArdle, M. J. Irwin, M. C. Jennings, R. J. Puddephatt, *Angew. Chem.* **1999**, *111*, 3571–3573; *Angew. Chem. Int. Ed*. **1999**, *38*, 3376–3378; i) M. Fujita, *Acc. Chem. Res.* **1999**, *32*, 53–61; j) H. W. Gibson, S.-H. Lee, *Can. J. Chem.* **2000**, *78*, 347–355; for catenane-like coordination interpenetrating networks see: k) S. R. Batten, R. Robson, *Angew. Chem.* **1998**, *110*, 1558–1595; *Angew. Chem. Int. Ed*. **1998**, *37*, 1460–1494; l) A. J. Blake, N. R. Champness, H. Hubberstey, W.-S. Li, M. A. Withersby, M. Schröder, *Coord. Chem. Rev.* **1999**, *183*, 117–138.

[2] C. O. Dietrich-Buchecker, J.-P. Sauvage, J.-M. Kern, *J. Am. Chem. Soc.* **1984**, *106*, 3043–3045; for the earliest $Cu^I$ catenate synthesis, involving a threaded intermediate complex, see: C. O. Dietrich-Buchecker, J.-P. Sauvage, J.-P. Kintzinger, *Tetrahedron Lett.* **1983**, *24*, 5095–5098.

[3] a) B. Mohr, M. Weck, J.-P. Sauvage, R. H. Grubbs, *Angew. Chem.* **1997**, *109*, 1365–1367; *Angew. Chem. Int. Ed. Engl*. **1997**, *36*, 1308–1310; b) M. Weck, B. Mohr, J.-P. Sauvage, R. H. Grubbs, *J. Org. Chem.* **1999**, *64*, 5463–5471.

[4] F. Bitsch, C. O. Dietrich-Buchecker, A.-K. Khémiss, J.-P. Sauvage, A. V. Dosselaer, *J. Am. Chem. Soc.* **1991**, *113*, 4023–4025.

[5] C. O. Dietrich-Buchecker, J.-P. Sauvage, J.-M. Kern, *J. Am. Chem. Soc.* **1989**, *111*, 7791–7800.

[6] a) C. Wu, P. R. Lecavalier, Y. X. Shen, H. W. Gibson, *Chem. Mater.* **1991**, *3*, 569–572; b) J.-C. Chambron, V. Heitz, J.-P. Sauvage, *J. Chem. Soc. Chem. Commun.* **1992**, 1131–1133.

[7] J.-P. Collin, P. Gavinã, J.-P. Sauvage, *J. Chem. Soc. Chem. Commun.* **1996**, 2005–2006.

[8] C. O. Dietrich-Buchecker, J. P. Sauvage, *Angew. Chem*. **1989**, *101*, 192–195; *Angew. Chem. Int. Ed. Engl*. **1989**, *28*, 189–192.

[9] N. Armaroli, L. De Cola, V. Balzani, J.-P. Sauvage, C. O. Dietrich-Buchecker, J.-M. Kern, A. Bailal, *J. Chem. Soc. Dalton Trans.* **1993**, 3241–3247.

[10] D. J. Cárdenas, A. Livoreil, J.-P. Sauvage, *J. Am. Chem. Soc.* **1996**, *118*, 11980–11981.

[11] The idea of using octahedral ligand geometries in catenate formation was actually proposed a decade *before* the Sauvage tetrahedral system was introduced (V. I. Sokolov, *Russ. Chem. Rev.* **1973**, *42*, 452–463). For more recent discussions of possible strategies to catenates based on metal templates with octahedral coordination preference, see: D. H. Busch, *J. Incl. Phenom*. **1992**, *12*, 389–395; N. V. Gerbeleu, V. B. Arion, J. Burgess, *Template Synthesis of Macrocyclic Compounds*, Wiley-VCH, Weinheim, **1999**.

[12] A. J. Blake, A. J. Lavery, T. I. Hyde, M. J. Schröder, *J. Chem. Soc. Dalton Trans.* **1989**, 965–970.

[13] A. L. Vance, N. W. Alcock, J. A. Heppert, D. H. Busch, *Inorg. Chem.* **1998**, *37*, 6912–6920.

[14] J.-P. Sauvage, M. Ward, *Inorg. Chem.* **1991**, *30*, 3869–3874.

[15] G. Rapenne, C. Dietrich-Buchecker, J.-P. Sauvage, *J. Am. Chem. Soc*. **1999**, *121*, 994–1001.

[16] C. A. Hunter, *Chem. Br.* **1998**, *34*(5), 17.

[17] a) D. A. Leigh, K. Moody, J. P. Smart, K. J. Watson, A. M. Z. Slawin, *Angew. Chem.* **1996**, *108*, 326–321; *Angew. Chem. Int. Ed. Engl.* **1996**, *35*, 306–310; b) T. J. Kidd, D. A. Leigh, A. J. Wilson, *J. Am. Chem. Soc.* **1999**, *121*, 1599–1600.

[18] D. A. Leigh, A. Murphy, J. P. Smart, M. S. Deleuze, F. Zerbetto, *J. Am. Chem. Soc.* **1998**, *120*, 6458–6467.

[19] The importance of these structural features for promoting catenate formation was exemplified by a very recent study which showed that it is not possible to produce octahedral catenates from terpy ligands which were not well preorganized for intracomponent cyclization (N. Belfrekh, C. Dietrich-Buchecker, J.-P. Sauvage, *Inorg. Chem*. **2000**, *39*, 5169–5172).

[20] Compound **2** was conveniently prepared in three steps from 4-hydroxybenzonitrile: 1) $HO(CH_2)_4CH{=}CH_2$, $Ph_3P$, DEAD, THF, 0°C, 59%; 2) $LiAlH_4$, THF, −78°C →reflux, 94%; 3) 2,6-pyridinedicarbaldehyde, MeOH, 92%.

[21] Compound **4** was conveniently prepared in three steps from 5-hexenyloxybenzylamine: 1) *t*$Boc_2O$, $NEt_3$, MeOH, 87%; 2) $[Ru(=CHPh)(PCy_3)_2Cl_2]$, $CH_2Cl_2$, Ar, RT, 24 h, 78%; 3) $CF_3CO_2H$, then $NEt_3$, $CH_2Cl_2$, 93%.

[22] [Zn{(*E*,*E*)-**1**}]$(ClO_4)_2$: $C_{62}H_{70}Cl_2N_6O_{12}Zn \cdot 0.5(C_2H_3N)$, $M_r = 1248.04$, crystal size $0.14 \times 0.08 \times 0.06$ mm, monoclinic $P2_1/c$, $a = 10.6258(5)$, $b = 17.4158(9)$, $c = 33.4757(18)$ Å, $\beta = 97.232(2)°$, $V = 6145.6(5)$ Å$^3$, $Z = 4$, $\rho_{calcd} = 1.349$ Mg m$^{-3}$; synchrotron radiation (CCLRC Daresbury Laboratory Station 9.8, silicon monochromator, $\lambda = 0.69280$ Å), $\mu = 0.553$ mm$^{-1}$, $T = 150(2)$ K. 22797 data (7081 unique, $R_{int} = 0.0489$, $1.65 < \theta < 21.00°$) were collected on a Siemens SMART CCD diffractometer using narrow frames (0.2° in $\omega$), and were corrected semiempirically for absorption and incident beam decay (transmission 0.83–1.00). The structure was solved by direct methods and refined by full-matrix least-squares methods on $F^2$ values of all data (G. M. Sheldrick, SHELXTL Manual, Version 5, Siemens Analytical X-ray Instruments, Madison, WI, **1994**) to give $wR = \{\Sigma[w(F_o^2 - F_c^2)^2]/\Sigma\{w(F_o^2)^2]\}^{1/2} = 0.2984$, conventional $R = 0.1087$ for $F$ values of 7081 reflections with $F_o^2 > 2\sigma(F_o^2)$, $S = 1.066$ for 761 parameters. Residual electron density extremes were 0.974 and −0.563 e Å$^{-3}$. The alkyl chains were modeled by using both geometrical and displacement parameter restraints. Hydrogen atoms were added in calculated positions and constrained to a riding model. Data for the copper catenate [Cu{(*E*,*E*)-**1**}]$(ClO_4)_2$ was collected and solved as above except: $C_{62}H_{71}CuN_6O_{12}$, $M_r = 1226.69$, crystal size $0.14 \times 0.10 \times 0.01$ mm, monoclinic $P2_1/c$, $a = 10.2948(6)$, $b = 17.4273(10)$, $c = 33.1511(18)$ Å, $\beta = 96.120(2)°$, $V = 5913.8(6)$ Å$^3$, $Z = 4$, $\rho_{calcd} = 1.378$ Mg m$^{-3}$; synchrotron radiation (CCLRC Daresbury Laboratory Station 9.8, silicon monochromator, $\lambda = 0.68950$ Å), $\mu = 0.528$ mm$^{-1}$, $T = 150(2)$ K. 10342 data (3460 unique, $R_{int} = 0.0784$, $1.93 < \theta < 16.50°$), correction for absorption and incident beam decay (transmission 0.9298–0.9947) $wR = \{\Sigma[w(F_o^2 - F_c^2)^2]/\Sigma[w(F_o^2)^2]\}^{1/2} = 0.3840$, conventional $R = 0.1556$ for $F$ values of 3460 reflections with $F_o^2 > 2\sigma(F_o^2)$, $S = 2.349$ for 339 parameters. Residual electron density extremes were 0.795 and −0.785 e Å$^{-3}$. Data for the cobalt catenate [Co{(*E*,*E*)-**1**}]$I_2$ was collected and solved as the others except: $C_{63}H_{70}CoI_2N_{6.5}O_4$, $M_r = 1294.99$, crystal size $0.14 \times 0.10 \times 0.01$ mm, monoclinic $P2_1/c$, $a = 10.2948(6)$, $b = 17.4273(10)$, $c = 33.1511(18)$ Å, $\beta = 96.120(2)°$. $V = 5913.8(6)$ Å$^3$, $Z = 4$, $\rho_{calcd} = 1.454$ Mg m$^{-3}$; synchrotron radiation (CCLRC Daresbury Laboratory Station 9.8, silicon monochromator, $\lambda = 0.68950$ Å), $\mu = 1.386$ mm$^{-1}$, $T = 150(2)$ K. 28253 data (5997 unique, $R_{int} = 0.1119$, $1.93 < \theta < 20.00°$), correction for absorption and incident beam decay (transmission 0.8296–0.9863), $wR = \{\Sigma[w(F_o^2 - F_c^2)^2]/\Sigma[w(F_o^2)^2]\}^{1/2} = 0.2662$, conventional $R = 0.1246$

  0044-8249/01/11308-1590 $ 17.50+.50/0 

for $F$ values of 5997 reflections with $F_o^2 > 2\sigma(F_o^2)$, $S = 1.215$ for 689 parameters. Residual electron density extremes were 0.955 and $-1.662$ e Å$^{-3}$. Crystallographic data (excluding structure factors) for the structures reported in this paper have been deposited with the Cambridge Crystallographic Data Centre as supplementary publication no. CCDC-147870 ([Zn{(*E*,*E*)-**1**}]$(ClO_4)_2$), CCDC-152441 ([Cu{(*E*,*E*)-**1**}]$(ClO_4)_2$), and CCDC-152442 ([Co{(*E*,*E*)-**1**}]$I_2$). Copies of the data can be obtained free of charge on application to CCDC, 12 Union Road, Cambridge CB21EZ, UK (fax: (+44) 1223-336-033; e-mail: deposit@ccdc.cam.ac.uk).

[23] The yields listed in Scheme 2 are yields after chromatography or recrystallization. Sometimes the mixture of olefin diastereomers complicates purification and, in particular, is a factor in the modest yields of [Co**1**]$L_2$ and [Ni**1**]$L_2$. The very low yield of [Hg**1**]$L_2$ by route (a) is caused by the lability of the ligands in the precursor complex [Hg**2**$_2$]$L_2$, which liberates free amine or imine in the reaction and prevents RCM occurring. All compounds gave satisfactory mass spectra, elemental analysis, IR, UV/Vis, and, with the exception of the paramagnetic catenates, $^{13}C$ and $^1H$ NMR data.

[24] S. Jurisson, D. Berning, W. Jia, D. Ma, *Chem. Rev.* **1993**, *93*, 1137–1156.

[25] D. Parker, *Chem. Br.* **1994**, 818–822.

[26] G. J. P. Britovsek, V. C. Gibson, D. F. Wass, *Angew. Chem.* **1999**, *111*, 448–468; *Angew. Chem. Int. Ed.* **1999**, *38*, 428–447.

[27] L. Douce, A. El-Ghayoury, A. Skoulios, R. Ziessel, *Chem. Commun.* **1999**, 2033–2034.

## Insertion of Helium and Molecular Hydrogen Through the Orifice of an Open Fullerene**

Yves Rubin,* Thibaut Jarrosson, Guan-Wu Wang, Michael D. Bartberger, K. N. Houk,* Georg Schick, Martin Saunders,* and R. James Cross*

*Dedicated to Professor Fred Wudl on the occasion of his 60th birthday*

One of the most exciting features of $C_{60}$ and the higher fullerenes is that their carbon cages have inner cavities large enough to hold any atom and even small molecules.[1, 2] The physical and chemical properties of these caged compounds (endohedral complexes) are determined by the degree of interaction established with the π-electron shell and the overall oxidation state of the complex.[3] As such, endohedral complexes offer a number of prospects for novel materials.[4–6] A large effort has been invested in finding efficient methods for the preparation and purification of these compounds.[1, 2, 7] So far, endohedral complexes have been formed with lanthanide or alkaline earth metals as charge transfer species,[1, 2] and with the rare gases[8, 9] or atomic nitrogen[10] as neutral complexes. Processes using the evaporation of graphite–metal oxide composites, as well as high-pressure and high-temperature or even high-energy plasma insertions into pure fullerenes, have been reported.[1–7] These methods constitute remarkable achievements and have already brought forth important insight into the properties of endohedral fullerene complexes. Nevertheless, they are still limited in scope and, more significantly, tend to give small amounts of material or meager incorporation fractions.

A stimulating prospect for the formation of these compounds can be described as a "molecular surgery" approach, which consists of the chemical creation of an opening within the fullerene cage (Figure 1a).[4] The opened species would allow the introduction of an atomic or molecular species, which could be followed by the "suturing" of broken bonds back onto the original framework. Each of these steps presents unique nontrivial challenges. The development of an effective method to open up the framework of $C_{60}$ by a one-pot reaction with bisazide **2**, to afford bislactam **1**,[11] provides an unprecedented opportunity for the preparation of endohedral complexes. We now report the successful insertion of two small neutral gases, helium and molecular hydrogen, into the fullerene bislactam derivative **1** which results in the highest incorporation fractions for any gas to date in a direct insertion process.

Bislactam **1** has currently the largest orifice formed in the shell of a fullerene with an inviting open-mouth shape.[4, 11] The amount of energy needed to push atoms or molecules through the orifice of **1** was first calculated using hybrid density functional theory. Activation barriers to insertion obtained as a function of guest size are listed in Table 1. The ground-state structures for empty bislactam **1**, its inclusion complexes of the inert gases He, $H_2$, Ne, $N_2$, and Ar, and the transition structures for their encapsulation were fully optimized at the B3LYP/3-21G level of theory, and energies were computed from these geometries using the 6-31G** basis set.[12]

The overall insertion processes for the smallest species (He, $H_2$) are predicted to be slightly endothermic (0.2–1.4 kcal mol$^{-1}$, Table 1). Patchkovskii and Thiel have investigated the encapsulation of helium by $C_{60}$ using MP2 calculations,[13] and found a favorable binding of 2.0 kcal mol$^{-1}$ as a result of van der Waals interactions of all sixty carbon atoms with the helium atom. These authors conclude that DFT calculations underestimate the exothermicity of He encapsulation within $C_{60}$ by about 3 kcal mol$^{-1}$ compared to the MP2 results, and thus the encapsulation of $H_2$ and He within the fullerene framework of **1** can be expected to be thermoneutral or slightly exothermic.

The predicted barrier for insertion of $H_2$ is nearly double that of helium, even though both species have similar van der Waals radii (1.20 and 1.22 Å, respectively).[14] The single imaginary vibrational modes at the transition states for

[*] Prof. Y. Rubin, Prof. K. N. Houk, T. Jarrosson, Dr. M. D. Bartberger, Dr. G. Schick
Department of Chemistry and Biochemistry
University of California, Los Angeles
Los Angeles, CA 90095-1569 (USA)
Fax: (+1) 310-206-7649
E-mail: rubin@chem.ucla.edu, houk@chem.ucla.edu
Prof. M. Saunders, Prof. R. J. Cross, Dr. G.-W. Wang[+]
Department of Chemistry
Yale University
New Haven, CT 06520 (USA)
Fax: (+1) 203-432-6144
E-mail: ms@gaus90.chem.yale.edu, james.cross@yale.edu
[+] Present address: Department of Chemistry
University of Science and Technology of China
Hefei, Anhui 230026 (PR China)

[**] This work was supported by grants from the National Science Foundation.